High-efficiency blue light generation at 426 nm in low pump regime

2016 J. Opt. 18 055506

(http://iopscience.iop.org/2040-8986/18/5/055506)

IOP Publishing Journal of Optics
J. Opt. 18 (2016) 055506 (8pp) doi:10.1088/2040-8978/18/5/055506

High-efficiency blue light generation at 426 nm in low pump regime

Jianfeng Tian[1], Chen Yang[1], Jia Xue[1], Yuchi Zhang[1,2], Gang Li[1] and Tiancai Zhang[1]

[1] State Key Laboratory of Quantum Optics and Quantum Optics Devices, Collaborative Innovation Center of Extreme Optics, Institute of Opto-Electronics, Shanxi University, Taiyuan, Shanxi 030006, People's Republic of China
[2] College of Physics and Electronic Engineering, Shanxi University, Taiyuan, Shanxi 030006, People's Republic of China

E-mail: yczhang@sxu.edu.cn and tczhang@sxu.edu.cn

Received 25 November 2015, revised 13 January 2016
Accepted for publication 1 February 2016
Published 24 March 2016

Abstract

We report high-efficiency Ti:sapphire-laser-based frequency doubling at the cesium D2 line 852 nm using a 20 mm-long periodically-poled potassium titanyl phosphate crystal in a bow-tie four-mirror ring enhancement cavity. The relatively complete cavity design procedure is presented. Focusing that is over twice as loose as optimal focusing is used, and both the fundamental frequency wave and second harmonic beam absorption-induced thermal lensing effects are weakened. Blue light of 210 mW at 426 nm, where absorption is severe, was obtained with 310 mW mode-matched fundamental light, corresponding to conversion efficiency of up to 67%. The blue light beam power showed 1.5% RMS fluctuation over 40 min.

Keywords: second harmonic generation, external enhancement cavity, thermal lensing effect

(Some figures may appear in colour only in the online journal)

1. Introduction

Frequency doubling of near-infrared light is an important method to obtain blue light, and this method has been widely used in many fields, including optical measurement [1], information storage and readout [2, 3], nonlinear optics [4, 5], quantum optics [6, 7], quantum information [6, 8] and other fundamental research fields in quantum physics. Specifically, those wavelengths that correspond exactly to atomic transitions are significant, because they provide various important quantum resources via optical parametric process for research of the interactions between nonclassical light and matter [9, 10], quantum metrology [11] and quantum storage [12, 13]. For example, one can improve the sensitivity of a magnetometer by probing atomic spin ensembles with a polarization-squeezed beam [14]. The primary key to this technology is an available, stable and powerful source of frequency doubling light sources as the pump of the optical parametric oscillator (OPO) to generate the vacuum squeezed state around the atomic transitions. For the typical OPO, the resonance threshold is about 200 mW and thus one needs the same order light power to pump the cavity [4, 13]. The significant alkali atomic transitions are usually near-infrared, and the frequency doublings of these lines are in blue or even ultra-violet regimes, which suffers seriously the absorption in many nonlinear crystals. Crystal heating due to the fundamental frequency wave with high intra-cavity circulating power and especially high absorption of the second harmonic beam limits both the mode matching efficiency and the performance of the second-harmonic generation (SHG). Obtaining a second-harmonic continuous wave source efficiently at relatively short wavelengths in the low pump regime remains an important issue.

The current technique of a high-quality blue beam generated by external cavity frequency doubling has been developed based on the use of nonlinear crystals placed in the enhancement cavity. To obtain high power and conversion efficiency of the second harmonic (SH), one can increase the pump power of the fundamental beam. In 1991, Polzik and Kimble obtained 650 mW of blue light at 430 nm with a pump power of 1.35 W using a $KNbO_3$ crystal in an optical ring cavity with conversion efficiency of 48%. Unfortunately,

$KNbO_3$ showed strong blue light-induced infrared absorption (BLIIRA) [15]. In 2007, Villa *et al* obtained 330 mW blue light at 426 nm using a ring cavity with a PPKTP crystal and a weakly focusing pump. The waist of the fundamental beam was approximately twice as large as the corresponding optimal beam size [16], and the conversion efficiency was as high as 55% at the mode matching fundamental power of 600 mW [17]. Recently, Marco Pizzocaro *et al* used a 1.3 W continuous wave titanium-sapphire laser at 798 nm with a LBO crystal in a ring cavity and got a SH power of 1.0 W and the conversion efficiency was 80% [18]. Due to the faint maximum single pass nonlinearity (of the order of $E_{NL} \approx 10^{-4}\ W^{-1}$), LBO crystal is only suitable for the frequency conversion of high pump power. However, low pumping is conducive to miniaturization of the SHG system, improvement the photothermal stabilization, and reduction the overall cost. Since the second harmonic power is quadratic to the incident fundamental wave (FW) power, the reduced FW power leads to a lower energy density inside the cavity, which usually causes the low conversion efficiency. To improve the efficiency, the experimental configuruations must be optimized. In 2003, with the moderate pump of 400 mW, an overall optical conversion efficiency of 60% was achieved at 423 nm by using a periodically-poled potassium titanyl phosphate (PPKTP) crystal. Because of the tight focusing inside the crystal, thermal-effect-induced bistability became a serious problem, and made it impossible to lock the cavity on a maximum for a long time. The thermal lensing effect also limits the mode-matching efficiency and must be taken into account in the experiments [19]. In 2005, a stable 461 nm blue light power of 234 mW with a net conversion efficiency of 75% at an input mode-matched power of 310 mW have been obtained [20]. However, it is challenging to double frequency at 852 nm corresponding to the cesium D2 line, for the generated harmonic lies in the band of more severe absorption of nonlinear materials [21]. Compared with the bow-tie configuration, standing-wave cavities provide a more compact and miniaturization design scheme with fewer optical components and thus lower losses. Irit Juwiler *et al* used a compact semimonolithic frequency-doubling cavity with PPKTP crystal, and achieved conversion efficiency of 56.5%, corresponding to a second-harmonic power of 117.5 mW at 532 nm with a continuous wave Nd:YAG pump power of 208 mW. It is worth mentioning that the second harmonic waves are generated in both the forward and backward directions, and it is necessary to carefully superpose these two waves constructively to obtain efficient frequency doubling [22]. By utilizing a monolithic PPKTP cavity, blue light generation at 426 nm by frequency doubling was also investigated but the conversion efficiencies were not good [23].

To obtain a relatively high conversion efficiency in the low pumping regime, it is necessary to improve the performance of the entire system, including the mode-matching efficiency of the pump beam, the frequency doubling cavity design, and the cavity stability. In the present work, we have comprehensively investigated the effects of optimal focusing conditions on the overall SHG conversion efficiency. The analysis shows that both the fundamental frequency wave and second harmonic beam absorption-induced thermal lens has a great influence on the mode matching efficiency, and the key point for improving the efficiency is to handle the beam waist in the doubler crystal experimentally. Our SHG system, which corresponds to the cesium atomic band, works with a maximum pump power of around 310 mW and deliberately adopts a significantly loose focusing regime to reduce thermal lensing effects. Consequently, we obtained 210 mW of blue light at 426 nm with a optical conversion efficiencies of up to 67%. The compact system is highly stable with low losses, and it is suitable for pumping of an optical parametric oscillator for various applications.

2. Theoretical analysis

For a frequency doubling ring cavity, the enhancement of the fundamental power on resonance is given by [15, 24]:

$$\frac{P_{c1}}{P_1} = \frac{T_1}{[1 - \sqrt{(1 - T_1)(1 - L_{loss})(1 - \Gamma P_{c1})}]^2}, \tag{1}$$

where P_1 is the mode-matching fundamental wave (FW) power. L_{loss} represents the intra-cavity FW round-trip losses excluding the transmission T_1 of the input coupler. These losses are mainly due to the absorption, scattering of the crystal and the imperfect coatings of the cavity mirrors. Γ includes all nonlinear losses and can be written in the form of $\Gamma = E_{NL} + \Gamma_{abs}$, where E_{NL} is the single pass conversion efficiency. The SH power is $P_2 = E_{NL} P_{c1}^2$. Γ_{abs} is the efficiency of the SH absorption process inside the crystal and the SH-absorbed power is $P_{abs} = \Gamma_{abs} P_{c1}^2$. $P_{c1} = \sqrt{P_1 \eta / E_{NL}}$ is the circulating FW power in the resonant cavity.

Based on equation (1), the overall conversion efficiency $\eta = P_2/P_1$ satisfies the following relation [19, 25]:

$$\sqrt{\eta}\left[2 - \sqrt{1 - T_1}(2 - L_{loss} - \Gamma\sqrt{\frac{\eta P_1}{E_{NL}}}\right]^2 - 4T_1\sqrt{E_{NL} P_1} = 0, \tag{2}$$

For a specified waist location at the center of the crystal, E_{NL} can be given by the well-known Boyd and Kleinman expression [16]:

$$E_{NL} = \frac{4 w_0^2 d_{eff}^2 L_C}{\varepsilon_0 c^3 \lambda_\omega n_\omega n_{2\omega}} h(\alpha, \xi, \sigma) \exp[-(\alpha_1 + \alpha_2/2) L_C], \tag{3}$$

$$h(\alpha, \xi, \sigma) = \frac{1}{2\xi} \int \int_{-\xi/2}^{+\xi/2} d\tau d\tau' \times \frac{\exp[-\alpha(\tau + \tau' + \xi) - i\sigma(\tau - \tau')]}{(1 + i\tau)(1 - i\tau)}, \tag{4}$$

where w_0 represents the Gaussian beam waist radius of FW beam at the crystal center. d_{eff} is the effective nonlinear optical coefficient. L_C is the nonlinear crystal length. n_ω and

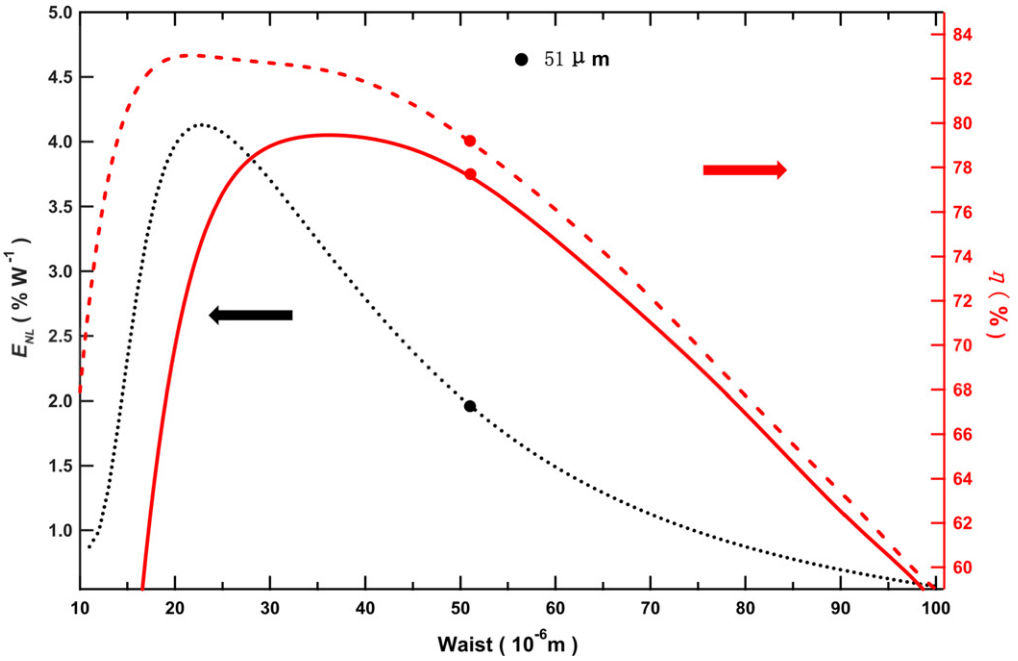

Figure 1. Single-pass conversion efficiency E_{NL} (black dotted line), theoretical overall conversion efficiency η versus beam waist w_0 at the crystal center without (red dashed line) and with (red solid line) thermal lensing effect using $P_1 = 310$ mW, $L_{\mathrm{loss}} = 1.3\%$ and $T_1 = 10\%$. The 'optimal' and experimentally adopted waists are 23 μm and 51 μm, respectively, corresponding to single-pass nonlinear conversion efficiencies of 4.2% W^{-1} and 1.96% W^{-1}, theoretical overall conversion efficiencies without thermal lensing effect of 83% and 79% and with thermal lensing effect of 75% and 78%.

$n_{2\omega}$ are the FW and SH refraction indices, respectively. ε_0 is the vacuum permittivity and c is the velocity of light in the vacuum. $\alpha = (\alpha_1 - \alpha_2)/2z_0$ and $\alpha_n\,(n = 1,\ 2$: FW, SH) are the linear absorption coefficients. h is the Boyd-Kleinman focusing factor, which depends on the focusing parameter $\xi = L_{\mathrm{C}}/z_0$ and the normalized wave-vector mismatch $\sigma = \Delta k z_0$, where $\Delta k = k_2 - 2k_1 - 2\pi/\Lambda$ and the Gaussian beam Rayleigh length $z_0 = kw_0^2$ and the wave-vector $k_{1,2} = 2\pi n_{\omega,2\omega}/\lambda_{\omega,2\omega}$. Λ represents the crystal grating period. Equations (3) and (4) show that the single pass coefficient E_{NL} is determined by the features of the nonlinear crystal d_{eff}, crystal length L_{C}, and the FW focusing inside the crystal, i.e., the value of the waist radius w_0. We have shown E_{NL} as a function of the beam waist w_0 in figure 1 (black dotted line). The parameters used here are $n_\omega = 1.84$, $n_2 = 1.94$, $\alpha_1 \approx 1\%\ \mathrm{cm}^{-1}$, $\alpha_2 \approx 10\%\ \mathrm{cm}^{-1}$, and crystal length $L_C = 20$ mm. The results show that the 'optimal' focusing waist is 23 μm, and this corresponds to the theoretical values of $\xi = 2.84$ and $E_{\mathrm{NL}} = 4.2\%\ \mathrm{W}^{-1}$.

Based on equation (2), the red dashed line in figure 1 displays the theoretical conversion efficiency η without considering thermal lensing effect when the beam waist varies in the range of $10\ \mu\mathrm{m} \leqslant w_0 \leqslant 100\ \mu\mathrm{m}$. It clearly shows that, due to the inevitable round trip passive losses,η undergoes significant change over the range of $20\ \mu\mathrm{m} \leqslant w_0 \leqslant 100\ \mu\mathrm{m}$. On the optimal focusing conditions, the theoretical conversion efficiency reaches a maximum value of 83% whereas at $w_0 = 60\ \mu$m the efficiency decreases to 76%. As the waist continues to increase, η will become even lower, which tells that it is necessary to choose the proper cavity waist in the range of $23\ \mu\mathrm{m} \leqslant w_0 \leqslant 60\ \mu\mathrm{m}$ for high conversion efficiency.

In addition, optical-absorption-induced thermal effect forms the thermal gradient inside the crystal and the thermal lensing effect affects both the mode matching and the quality of the generated beam. A simple analytical model of a thermal lens can be obtained using a thin lens placed in the middle of the crystal. The dioptric power of thermal lens can then be expressed as [26]:

$$P_{th} = \frac{1}{f_{th}} = \frac{1}{f_{w1}} + \frac{1}{f_{w2}}, \tag{5}$$

where f_{w1} and f_{w2} are the focal lengths of the thermal lens with respect to the absorption of the fundamental and frequency-doubled beams, respectively, and [27]:

$$f_{wi} = \frac{\pi K_{\mathrm{c}} w_i^2}{P_{ci}(dn/dT)}\left(\frac{1}{1 - \exp(-\alpha_i L_{\mathrm{C}})}\right) \quad (i = 1,\ 2\text{: FW, SH}), \tag{6}$$

where $dn/dT = 15.3 \times 10^{-6}\ \mathrm{K}^{-1}$ is the coefficient of refractive index change with temperature and $K_{\mathrm{c}} = 3.3\ \mathrm{W/(m\ ^\circ C)}$ is the thermal conductivity of the KTP crystal. The circulating fundamental beam power in the resonant cavity is $P_{c1} = \sqrt{P_1\eta/E_{\mathrm{NL}}}$, where P_1 is the fundamental wave power which is approximately 310 mW in our experiment.

To evaluate f_{w2}, we assumed that $P_{c2} = P_2$ in equation (6). Because the SH is not homogeneous along the length of the crystal ($P_2 = 0$ at $z = 0$, and P_2 is a maximum at $z = L_{\mathrm{C}}$), equation (6) can only be used to estimate f_{w2} with the blue beam waist $w_{02} = w_0/\sqrt{2}$ [20]. As shown in

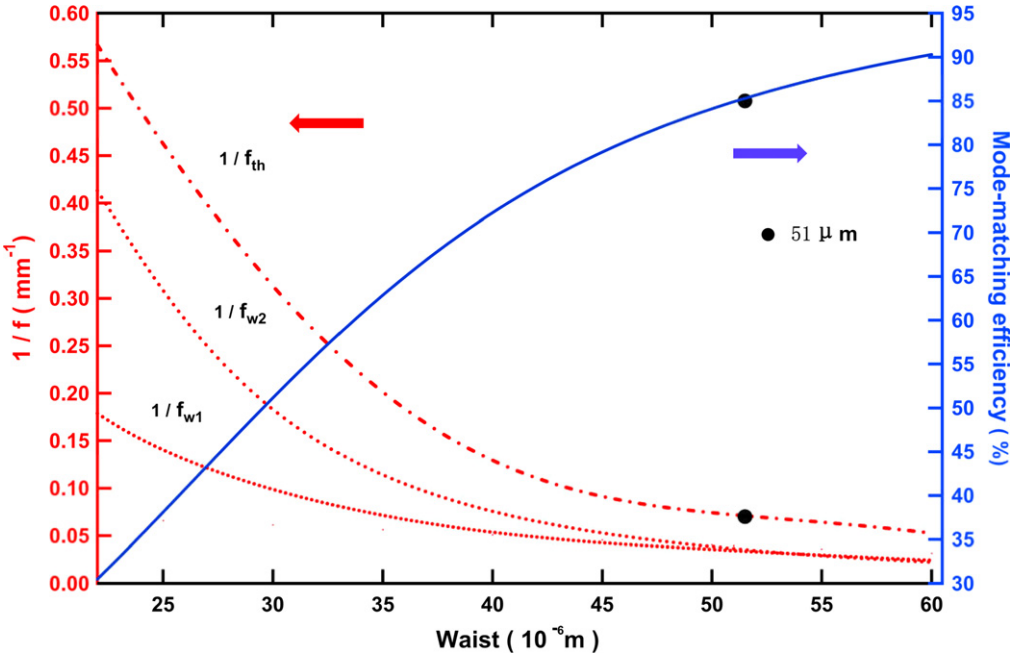

Figure 2. Thermal lens power ($1/f$) and theoretical mode-matching efficiency M versus pump beam waist w_0 at the crystal center when the fundamental wave power is 310 mW. The red dot-dashed line is the thermal lens power. The two red dotted lines represent the FW and SH absorption induced thermal lens power, respectively. The blue solid line is the theoretical mode-matching efficiency. The adopted cavity waist is 51 μm, which gives a thermal lens focal length of 14.3 mm, and the theoretical mode-matching efficiency is 85%.

figure 2, the power of the thermal lens is sensitive to the pump beam waist size in the range of 23 μm $\leqslant w_0 \leqslant$ 60 μm, even in the low pump power regime. Pump mode-matching losses occur due to the thermal lensing effect and these losses can be estimated simply by calculating the overlap integral between the TEM_{00} modes of the incident beam and the cavity eigenmodes [28]:

$$M = \frac{16\prod_{\beta=x,y}\left\{\int_0^l \frac{1}{\omega_{\beta,1}^2(z)+\omega_{\beta,e}^2(z)}dz\right\}^2}{\prod_{\beta}\left\{\int_0^l \frac{1}{\omega_{\beta,1}^2(z)}dz\right\}\left\{\int_0^l \frac{1}{\omega_{\beta,e}^2(z)}dz\right\}}, \tag{7}$$

where M is the FW mode-matching efficiency, $w_1(z)$ is the FW beam radius at $1/e$ of the amplitude, $w_e(z)$ are that of the cavity eigenmodes, and

$$w(z) = w_0\sqrt{1+\left(\frac{z}{z_0}\right)^2}. \tag{8}$$

The blue solid line in figure 2 shows the change in the mode-matching efficiency with increasing waist on low pump conditions. For $w_0 = 60$ μm of the loose focusing regime the matching efficiency is close to 91%, while for 'optimal' focused in tight focusing regime it is reduced to 32%. Strong focusing results in larger mode-matching losses of the input pump power, which leads to the reduced final frequency conversion efficiency. Therefore, to obtain high SH efficiency, weak focusing conditions are necessary to reduce the thermal effects. The red solid line in figure 1 shows the theoretical overall conversion efficiency when considering the thermal lens effects. It is clearly seen that η changes relatively slightly from 74.5% to 79.5% over the range of 23 μm $\leqslant w_0 \leqslant$ 60 μm. Based on the above analysis, and taken into account other thermally-induced effects in the SHG process, such as thermal dispersion, thermal stress, thermally-induced phase mismatching, in the experiment we choose a cavity waist of about 51 μm, which corresponds to $\xi = 0.57$ and $E_{\mathrm{NL}} = 1.96\%\ \mathrm{W}^{-1}$. The conversion efficiency in this case is about 78% theoretically.

Finally, optical impedance matching is also an important issue that must be considered in this process. The coupling coefficient of the input coupler can be optimized for the total losses, including the linear and nonlinear losses, for a given pump power P_1 and nonlinearity E_{NL}. The optimal transmission T_1^{opt} of the input coupler can then be expressed as [19, 25]:

$$T_1^{\mathrm{opt}} = \frac{L_{\mathrm{loss}}}{2} + \sqrt{\frac{L_{\mathrm{loss}}^2}{4} + \Gamma \cdot P_1}, \tag{9}$$

and

$$\Gamma = E_{\mathrm{NL}} + \Gamma_{\mathrm{abs}} = E_{\mathrm{NL}} + E_{\mathrm{NL}}(\exp[\alpha_2 \times L_C/2] - 1). \tag{10}$$

Based on the FW power in our experiment of 310 mW, $L_{\mathrm{loss}} = 1\%$–3%, and $E_{\mathrm{NL}} = 1.5\%$–$2\%\ \mathrm{W}^{-1}$, so the optimal T_1^{opt} is 8%–10%.

3. Experimental setup

A schematic of the experimental setup is shown in figure 3. A continuous-wave (CW) single longitudinal-mode Ti:sapphire

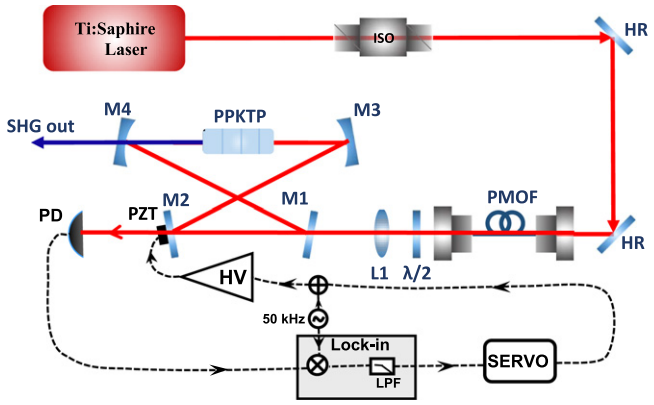

Figure 3. Schematic of the experimental setup. ISO: Faraday isolator; PMOF: polarization-maintaining optical fiber; HWP: half-wave plate; L1: focusing lens, $f = 500$ mm. In the electronics section: Lock-in: lock-in amplifier, PD: photodetectors, HV: high-voltage amplifier, LPF: low-pass filter.

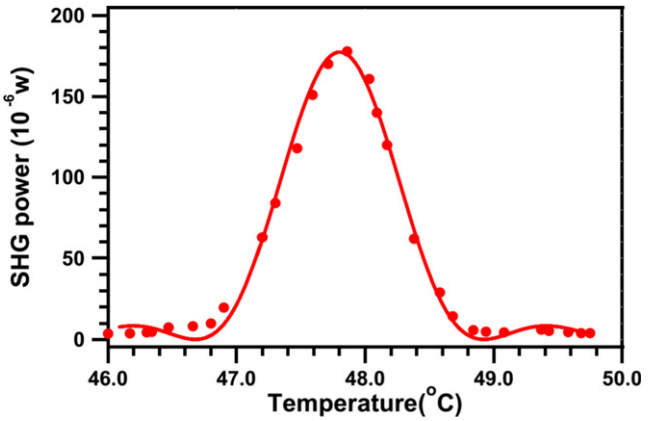

Figure 5. Measured temperature tuning curve with fitting in a single-pass configuration. The incident FW power is 110.5 mW and the temperature bandwidth is $\Delta T_{\mathrm{FWHM}} = 0.93$ °C.

laser, which is locked at the D2 transition of cesium atoms, provides the pump beam. A 30 dB isolator is used to eliminate back-reflected light. The beam is mode cleaned by a polarization-maintaining single-mode fiber and mode matched into the OPO by lens L1. The measured mode-matched efficiency is approximately 94%, and the cavity mode is the TEM_{00} single longitudinal mode. A half-wave plate is used to adjust the pump beam polarization to match it to the crystal axis.

We have used a symmetrical bow-tie ring cavity containing a PPKTP nonlinear crystal. This PPKTP crystal offers some significant advantages, including a large nonlinear coefficient, which is suitable for doubling in the low power regime, an absence of walk-off, which limits the efficiency and creates an astigmatic beam, reduced sensitivity to photorefractive optical damage, and no BLIIRA [19]. The PPKTP crystal (manufactured by Raicol) has dimensions of 1 mm × 2 mm × 20 mm with first-order poling for type I quasi-phase matching. The crystal poling period is approximately 4 μm. Both end surfaces are antireflection-coated for both the fundamental and SH wavelengths. The crystal is mounted in a homemade copper oven that is controlled by a temperature controller (ITC502, Thorlabs, Inc.). The cavity consists of two planar mirrors, M1 and M2, and two concave-convex mirrors, M3 and M4, that have a radius of curvature of 100 mm. We choose transmission of 10% for the input coupler mirror M1, and a PZT is bonded to the highly reflective mirror M2 (reflectivity of 99.9% at the fundamental wavelength) which is then used to control the cavity length. The curved mirrors M3 and M4 are super mirrors with reflectivity of 99.9998% at 852 nm and a transmission coefficient of 78% at 426 nm. The total cavity length is approximately 489 mm with a folding angle of 5.2 degrees, which leads to negligible astigmatism [29]. The distance between

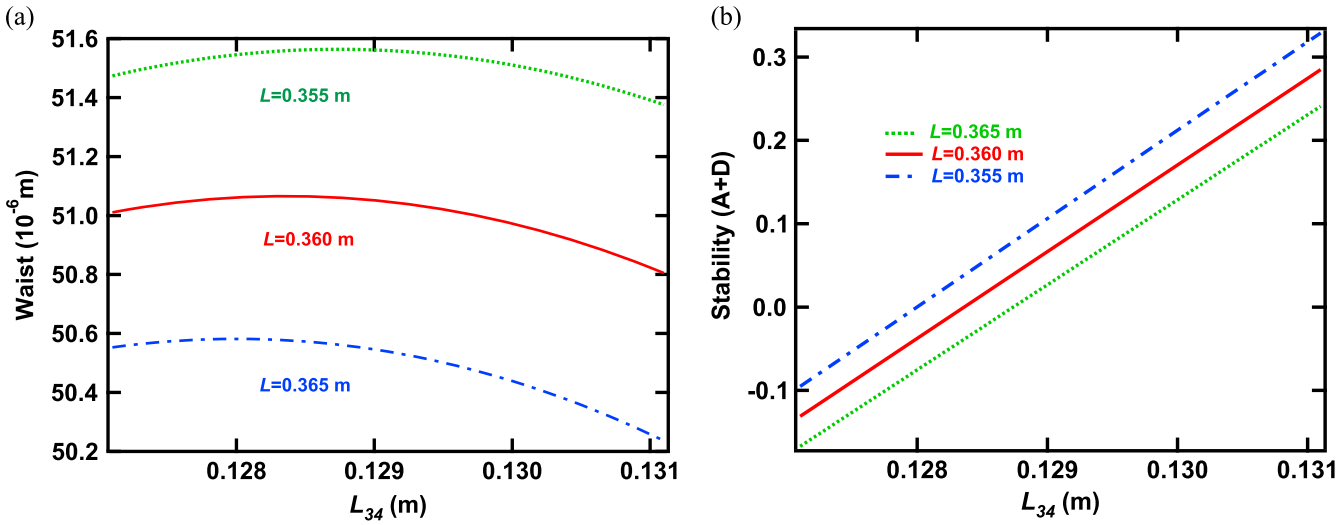

Figure 4. Cavity eigenmode waist (a) and A + D parameter (b) as function of the distance L_{34} under three different length L (0.355 m, 0.360 m and 0.365 m). L_{34} is the direct distance between concave mirrors M3 and M4. L represents the total cavity length, except for L_{34}. Green, red and blue lines are for $L = 0.355$ m, 0.360 m and 0.365 m. In our experiments, the designed values of L_{34} and L are 129 mm and 360 mm, respectively. The cavity eigenmode waist radius is 51 μm and $A + D = 0.06$.

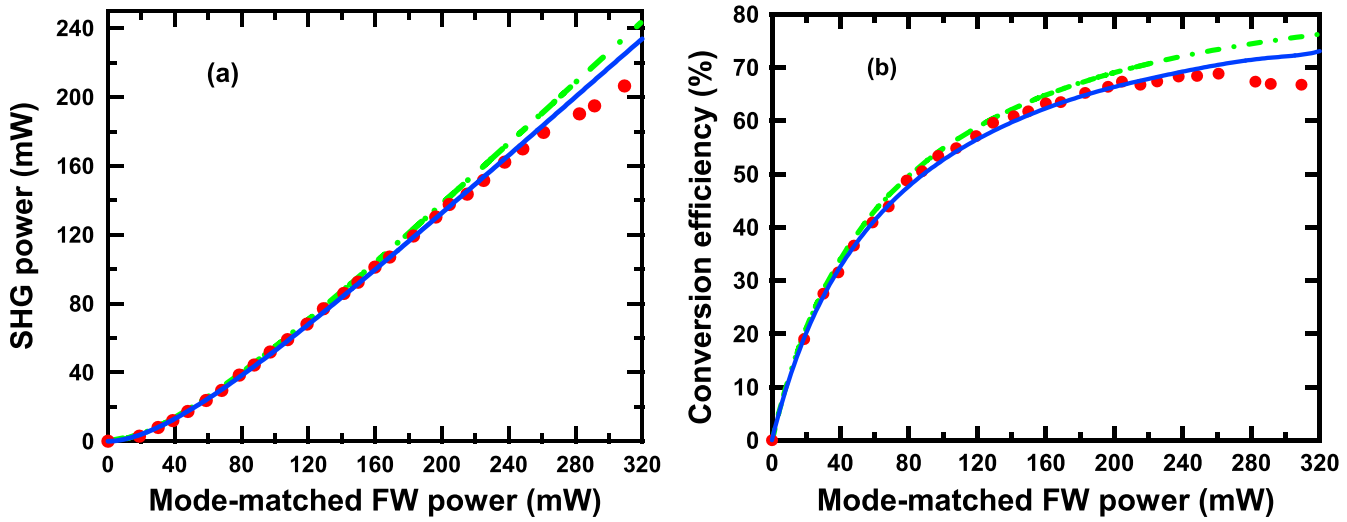

Figure 6. (a) SHG power P_2 and (b) conversion efficiency η as a function of the mode-matched FW power P_1. Green dot-dashed and blue solid lines are the theoretical results without and with thermal lens effects, respectively. The experimental parameters used are, $w_0 = 51\ \mu$m, $E_{NL} = 1.45\%\ W^{-1}$, $L_{loss} = 1.3\%$, $\Gamma_{abs} = 0.1E_{NL}$, $T_1 = 10\%$. Red dots represent experimental results.

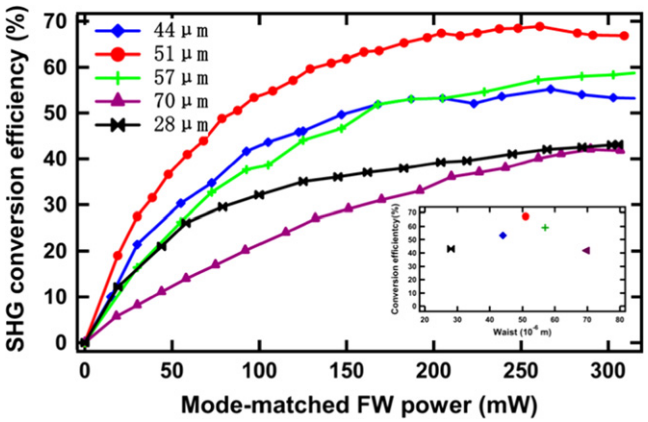

Figure 7. SHG conversion efficiency η as a function of mode-matched FW power P_1 for various cavity eigenmode waist radius of 28 μm, 44 μm, 51 μm, 57 μm and 70 μm. The inset shows the corresponding highest conversion efficiency is 43.1%, 53.1%, 67.3%, 59.1% and 41.8%, respectively, where the FW power is about 310 mW.

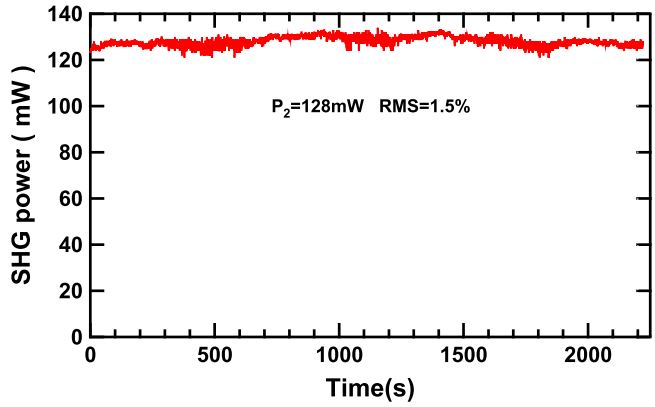

Figure 8. Power stability of the SH output over 40 min. The RMS fluctuation is 1.5%. Under the condition of incident FW power of approximate 240 mW, while the SHG power is 128 mW.

M3 and M4 is 129 mm. Based on the ABCD-matrix method for Gaussian beams, figures 4(a) and (b) show the crystal center waist radius and the resonant cavity stability as a function of the distance between mirror M3 and M4, respectively. It can be seen that, in the actual experiment, the eigenmode waist does not change very much when L_{34} varies in a few millimeters and the cavity is in the stable range with $|A + D| \leqslant 2$ [30]. When considering the thermal lensing effect under our experimental conditions of $P_1 = 310$ mW and $w_0 = 51\ \mu$m, the value of $|A + D|$ changes from 0.06 to 0.07, which means that our frequency doubling cavity still retains adequate 'stability margin' [31]. This well-designed system can improve the SHG power stability.

4. Experimental results and discussions

To characterize the PPKTP crystal, we measured the SH output power transmitting through M4 in a single-pass configuration as a function of temperature by removing the input coupler (M1). The focusing is the same as the actual resonant situation. We finish the measurement sequence at a low incident fundamental wave power of 110.5 mW to reduce any unwanted contributions from the thermal effects. The temperature changes from 46 °C to 49.4 °C. The maximum SHG power of 177 μW is generated at the best phase matching temperature of 47.8 °C, and this corresponds to $E_{NL} = 1.45\%\ W^{-1}$, which means the effective nonlinear coefficient of $d_{eff} = 6.93\ pm V^{-1}$ and such a value is comparable to those coefficient measured elsewhere (5–8 pm V^{-1}) from OPO threshold measurement or difference frequency generation [20, 32], even when wavelength dispersion is accounted for. The result is shown in figure 5, together with a fitting curve (red solid line). The full-width at half-maximum bandwidth is $\Delta T_{FWHM} = 0.93$ °C [33].

The cavity length is locked by using the standard phase-sensitive dither-and-lock method. A dither modulation is applied to the piezoelectric transducer mounted on M2 and the bandwidth of the servo loop is about 10 kHz (see figure 3) [34]. When the cavity is locked, we can measure both the SHG power and the conversion efficiency with respect to the incident fundamental wave power. The results are shown in figure 6. The red dots indicate the measured results, while green dot-dashed and blue solid lines are the theoretical calculation without and with thermal lens effect, respectively. Here, the intra-cavity loss L_{loss} is measured to be 1.3% [35]. A maximum SHG power of 210 mW is obtained for the input mode-matched FW power of 310 mW, which corresponds to a conversion efficiency of 67%. The obtained results are in good agreement with the theory when the pump power is relatively low and the thermal effect is considered. When the pump power increases to more than 270 mW, there are some discrepancies between the theoretical and experimental results. These discrepancies may be attributed to the residual blue-absorption-induced thermal effect. This residual heating effect will change the cavity length and form a thermal gradient inside the crystal, destroying the previous focusing conditions, and thus affecting the fundamental beam propagation and reducing the mode-matching efficiency.

We have tested other four different cavities with different eigenmode waist radius of 28 μm, 44 μm, 57 μm and 70 μm, respectively. The experimental results are shown in figure 7. The best results were obtained with waist of 51 μm and this shows that by using over twice as loose as optimal focusing, the absorption-induced thermal lensing effects is minimized while still maintaining the satisfying overall conversion efficiency. This result is consistent with our theoretical analysis.

Finally, the SH output power stability is measured at 128 mW for over 40 min in CW mode. The results are shown in figure 8. The root mean square (RMS) fluctuation is 1.5%. This fluctuation should partly be attributed to the slow variation of the FW power and residual absorption-induced thermally dephasing at higher power operation.

5. Conclusion

We have generated blue light at 426 nm by high-efficiency frequency doubling of the output of a Ti:sapphire laser working at a low pump level. A PPKTP crystal is placed in a bow-tie four-mirror ring enhancement cavity. A maximum blue light power of 210 mW is obtained from a mode-matched fundamental wave power of approximately 310 mW, and the measured conversion efficiency is about 67%. The SHG stability is measured at 128 mW, and gives an RMS fluctuation value of 1.5% over about 40 min. We analyzed the effect of the beam waist and confirmed that weak focusing and a well-designed cavity enable us to reduce the thermal effect and improve the performance of the frequency doubler. In the low pump regime, SHG is mainly limited by the intra-cavity losses. This stable and high-efficiency frequency doubling system is suitable for many applications in quantum state generation at atomic transitions, laser spectroscopy, and atom lithography.

Acknowledgments

This work was supported by the Major State Basic Research Development Program of China (Grant No. 2012CB921601) and the National Natural Science Foundation of China (Grant Nos. 61227902, 91336107 and 61275210). YCZ is also supported by the Natural Science Foundation of Shanxi (Grant No. 2014021011-2).

References

[1] Polzik E S, Carri J and Kimble H J 1992 *Phys. Rev. Lett.* **68** 3020
[2] Hesselink L, Orlov S S, Liu A, Akella A, Lande D and Neurgaonkar R R 1998 *Science* **282** 1089
[3] Ditlbacher H, Lamprecht B, Leitner A, Aussenegg F R and Aussenegg F R 2000 *Opt. Lett.* **25** 563
[4] Suzuki S, Yonezawa H, Kannari F, Sasaki M and Furusawa A 2006 *Appl. Phys. Lett.* **89** 061116
[5] Wang F Y, Shi B S, Chen Q F, Zhai C and Guo G C 2008 *Opt. Commun.* **281** 4114
[6] Neergaard-Nielsen J S, Nielsen B M, Hettich C, Mølmer K and Polzik E S 2006 *Phys. Rev. Lett.* **97** 083604
[7] Ou Z Y and Lu Y J 1999 *Phys. Rev. Lett.* **83** 2556
[8] Zhang T C, Goh K W, Chou C W, Lodahl P and Kimble H J 2003 *Phys. Rev.* A **67** 033802
[9] Hald J, Sørensen J L, Schori C and Polzik E S 1999 *Phys. Rev. Lett.* **83** 1319
[10] Turchette Q A, Georgiades N P, Hood C J, Kimble H J and Parkins A S 1998 *Phys. Rev.* A **58** 4056
[11] Eberle T, Steinlechner S, Bauchrowitz J, Händchen V, Vahlbruch H, Mehmet M, Müller-Ebhardt H and Schnabel R 2010 *Phys. Rev. Lett.* **104** 251102
[12] Appel J, Figueroa E, Korystov D, Lobino M and Lvovsky A I 2008 *Phys. Rev. Lett.* **100** 093602
[13] Burks S, Ortalo J, Chiummo A, Jia X, Villa F, Bramati A, Laurat J and Giacobino E 2009 *Opt. Express* **17** 3777
[14] Wolfgramm F, Cerè A, Beduini F A, Predojević A, Koschorreck M and Mitchell M W 2010 *Phys. Rev. Lett.* **105** 053601
[15] Polzik E S and Kimble H J 1991 *Opt. Lett.* **16** 1400
[16] Boyd G D and Kleinman D A 1968 *J. Appl. Phys.* **39** 3597
[17] Villa F, Chiummo A, Giacobino E and Bramati A 2007 *J. Opt. Soc. Am.* B **24** 576
[18] Pizzocaro M, Calonico D, Pastor P C, Catani J, Costanzo G A, Levi F and Lorini L 2014 *Appl. Opt.* **53** 3388
[19] Goudarzi F T and Riis E 2003 *Opt. Commun.* **227** 389
[20] Targat R L, Zondy J J and Lemonde P 2005 *Opt. Commun.* **247** 471
[21] Hansson G, Karlsson H, Wang S H and Laurell F 2000 *Appl. Opt.* **39** 5058
[22] Juwiler I and Arie A 2003 *Appl. Opt.* **42** 7163
[23] Deng X, Zhang J, Zhang Y C, Li G and Zhang T C 2013 *Opt. Express* **21** 25907
[24] Ashkin A, Boyd G D and Dziedzic T M 1966 *IEEE J. Quantum Electron.* **QE–2** 109
[25] Han Y S, Wen X, Bai J D, Yang B D, Wang Y H, He J and Wang J M 2014 *J. Opt. Soc. Am.* B **31** 1942
[26] Hecht E 2002 *Optics* (Reading, M A: Addison-Wesley)
[27] Innocenzi M E, Yura H T, Fincher C L and Fields R A 1990 *Appl. Phys. Lett.* **56** 1831

[28] Uehara N, Gustafson E K, Fejer M M and Byer R L 1997 *Proc. SPIE* **2989** 57
[29] Vainio M, Peltola J, Persijn S, Harren F J M and Halonen L 2009 *Appl. Phys.* B **94** 411
[30] Siegman A E 1986 *Lasers* (Mill Valley, CA: University Science Books)
[31] Franklin G F, Powell J D and Emami-Naeni A 2015 *Feedback Control of Dynamic Systems* (Reading, MA: Addison-Wesley)
[32] Lundeman J H, Jensen O B, Andersen P E, Engels S A, Sumpf B, Erbert G and Petersen P M 2008 *Opt. Express* **16** 2486
[33] Kumar S C, Samanta G K and Ebrahim-Zadeh M 2009 *Opt. Express* **17** 13711
[34] Hamilton C E 1992 *Opt. Lett.* **17** 728
[35] Li G, Zhang Y C, Li Y, Wang X Y, Zhang J, Wang J M and Zhang T C 2006 *Appl. Opt.* **45** 7628